Applied Acoustics 74 (2013) 1511–1518

Contents lists available at SciVerse ScienceDirect

Applied Acoustics

journal homepage: www.elsevier.com/locate/apacoust

The development of a non-surgical direct drive hearing device with a wireless actuator coupled to the tympanic membrane

Yu-Lin Song [a,b], Jhong-Ting Jian [c], Wei-Zen Chen [c], Chih-Hua Shih [a], Yuan-Fang Chou [a], Tien-Chen Liu [d], Chia-Fone Lee [e,f,*]

[a] Department of Mechanical Engineering, National Taiwan University, Taipei, Taiwan
[b] High Technology Research Center, Yen Tjing Ling Industrial Research Institute, Taipei, Taiwan
[c] Department of Electronics Engineering, National Chiao-Tung University, Hsinchu, Taiwan
[d] Department of Otolaryngology, National Taiwan University Hospital, Taipei, Taiwan
[e] Department of Otolaryngology, Tzu Chi General Hospital, Hualien, Taiwan
[f] Department of Medicine, Tzu Chi University, Hualien, Taiwan

ARTICLE INFO

Article history:
Received 16 October 2012
Received in revised form 1 May 2013
Accepted 21 June 2013
Available online 18 July 2013

Keywords:
Hearing aids
Wireless
Actuator
Electromagnetic
Finite element analysis

ABSTRACT

A non-surgical, direct driving hearing device with an actuator placed on the tympanic membrane was designed, fabricated and tested. The actuator consisted of two photodiodes, an aluminum ring, two neodymium iron permanent magnets, two opposing wound coils, a latex membrane and a Provil Novo™ membrane. The transducer coupled to the ear drum-utilizing photodiodes and permanent magnets on the motive components could eliminate the need for electrical connections to the moving components. An optic probe was designed to allow sound and light signals to enter the ear canal. By using opto-electromagnetic coupling, the developed hearing device could transmit information over a distance without using cables. The wireless actuator was achieved by two configurations: in one, two light emitting diodes were used for carrying the input signals, and in the other, the corresponding photodiodes were used for receiving the light signals and generating the currents in the actuator. The wireless actuator was designed to use light to carry energy and transmit the signals; thus, the occlusion effect created by traditional ear molds could be avoided. Finally, the wireless actuator was fabricated and tested with a laser Doppler vibrometer. The actuator showed displacements of vibration between 30–0.2 nm and from 400 Hz to 7 kHz with reduced vibration at higher frequencies. The gain of the actuator with 120 μA on the umbo displacement was approximately 3–13 dB from 400 to1500 Hz and decreased to 6 dB between 1500 Hz to 3 kHz and down to −1 to −6 dB above 3 kHz. Distortions of the umbo vibration amplitude were approximately −1 to −10 dB across frequencies. The results suggest that light can transmit the sound signal remotely and that adequate amplification can be achieved by this actuator. The reduced amplitude above 3 kHz was a consequence of the mass effect of the actuator, which should be miniaturized in the future.

1. Introduction

Hearing impairment affects approximately 28 million individuals, or approximately 1 in 10, in the United States and becomes more prevalent with age [1]. It is estimated that of those older than 65 years of age, 31.4% are hearing impaired. These percentages are expected to rise with increased age. Only 5% of hearing-impaired individuals have a conductive hearing loss that requires simple amplification to increase loudness and could be treated medically or surgically. The remaining 95% have a sensorineural hearing loss that is a much more complex problem for amplification. The effects of such a loss are multidimensional and can be characterized by changes in the attenuation and distortion of acoustic inputs [2]. Attenuation can be viewed as a quantitative effect and reflects the loss of auditory sensitivity [3]. Distortion is a qualitative effect in hearing loss. When a sound is heard, its quality might be poorer than that heard by a normal person. Hearing devices have long been the principal method of treatment and alleviation for sensori-neural hearing impairment. Candidates for a hearing aid are anyone, adult or child, who is having communication problems related to hearing. The past decade has seen many advances in hearing aid technology and performance.

Although conventional hearing aids have improved tremendously throughout with miniaturization and improvements in digital signal processing over the last decade, some people do not fully benefit from the improved devices [4]. These disadvantages arise from several reasons that may include the distortion of sound

* Corresponding author. Address: Department of Otolaryngology, Buddhist Tzu Chi General Hospital, No. 707, Sec. 3, Chung Yang Rd., Hualien 970, Taiwan, R. O. C. Fax: 886 3 8560977; mobile: 886 919 510591.
E-mail address: e430013@yahoo.com.tw (C.-F. Lee).

0003-682X/$ - see front matter
http://dx.doi.org/10.1016/j.apacoust.2013.06.014

quality, feedback, occlusion of the ear canal or physical discomfort that is caused by those devices [5,6]. The position of the hearing aid in the auricle and external ear canal can not only block sound transmission but also interfere with normal resonances and frequency amplification [7]. Further distortion occurs when the electronic signals are converted back into acoustic signals through the output receivers. In addition, acoustic feedback is another problem with conventional hearing devices. The output from the device is picked up by the input microphone from sound transmitting back into it between the device and the ear canal [1,7]. There is also an acoustic occlusion effect with conventional hearing aids. This is a phenomenon in which sounds cannot dissipate normally and give rise to the annoying perception of one's own voice sounding more hollow and louder than normal. During vocalization, bone-conducted energy results in vibration of the mandible and soft tissue in close proximity to the external ear canal [8]. For some closed vowels, occluding the external ear canal using a shallow insertion depth can result in levels of 100 dB SPL within the canal [9]. Patient dissatisfaction resulting from the occlusion effect can lead to inconsistent hearing aid or rejection [8,9]. Dillon et al., revealed that 27.8% of patient experienced problems related to the quality of their voice [10]. The distortion of sound quality and feedback may, at least partially, be circumvented by placing a magnet on the tympanic membrane [11–13]. Examples for the realization of these ideas are the " in the canal" hearing aid with an electromagnetic coil driving a samarium-cobalt magnet attached to the umbo by the Smith & Nephew Richard Company (Memphis, TN, and UK) and the Earlens system of Perkins, which contains a magnetic actuator on the ear drum [7]. To address the aforementioned problems of hearing aids, in 1996, Perkins [7] developed an Earlens system with a magnetic actuator on the ear drum. Unfortunately, the functional gains of this system were variable, and the magnetic forces were quickly decreased with increased distance. Additionally, a slight shift in the position of the coil in the external ear canal lead to alterations in the distance and the direction of the magnetic field resulting in unpredictable or insufficient power output.

The use of light for signal transduction has been implemented in many fields. For example, a retinal prosthesis is a rehabilitative implantable device that is designed to restore a limited form of vision to blind individuals who suffer from retinal degenerative diseases [14,15]. This dual unit device employs an external unit to capture visual information that is transmitted via a wireless telemetry link to the unit implanted in the eyeball or intraocular unit.

The developed hearing device transmits information over a distance without the use of cables. The wireless vibration actuator can be attached onto the tympanic membrane (TM). The electric wires are wound around the magnet on the actuator. This design minimizes the current required to drive the magnet and provides stable vibration. Furthermore, to leave the canal open, the input sound signals are carried and transmitted remotely from the signal processor to the actuator with an infrared light photo-diode (PD) and an ambient light photo-diode (PD) to overlap with the spectrum. The light emitted from two light emitting diodes (LEDs) then reaches the two corresponding photodiodes (PDs), which generate currents to drive the electromagnetic actuator. The wireless actuator works by using opto-electromagnetic coupling. Therefore, sounds could be amplified and converted to allow for the direct vibration of auditory ossicles.

2. Materials and methods

2.1. Design of the actuator

A new type of wireless actuator was designed to be attached to the TM as shown in Fig. 1(a). The actuator consisted of two photodiodes, two permanent magnets, an aluminum ring, two wound coils, a latex membrane and a Provil Novo™ membrane (Heraeus Kulzer, New York, USA) as demonstrated in Fig. 1(b). The thickness of the latex membrane was approximately 0.1 mm. The Provil Novo™ membrane was used to fit the conical concavity of the TM. The actuator was placed on the umbo area of the TM, and mineral oil was used to maintain the position of the actuator. Thus, the adhesive forces between the TM and the Provil membrane were provided by the mineral oil [7]. The electromagnetic vibration actuator consisted of two parts: the electromagnetically actuating part and the mechanically vibrating parts. The electromagnetic driving parts are composed of two wound coils and a permanent magnet. The mechanically vibrating parts are composed of a latex membrane and a Provil Novo™ membrane (Heraeus Kulzer, New York, USA).The control parameters for the vibration actuators are the intensity of the electrical current, the number of coil turns, the signal frequency, and the size and mass of the magnets and

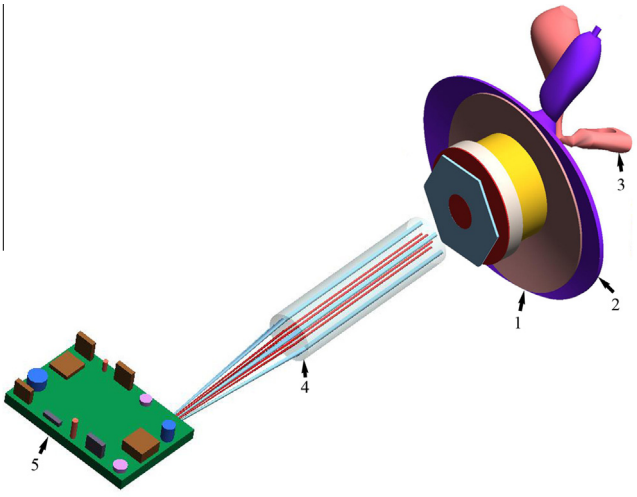

Fig. 1a. A diagram of the wireless vibration actuator (1) to be put onto the tympanic membrane (2). The tympanic membrane (2) was connected to the ossicles (3). The light probe (4) and the signal processor together as a complete amplification device (5).

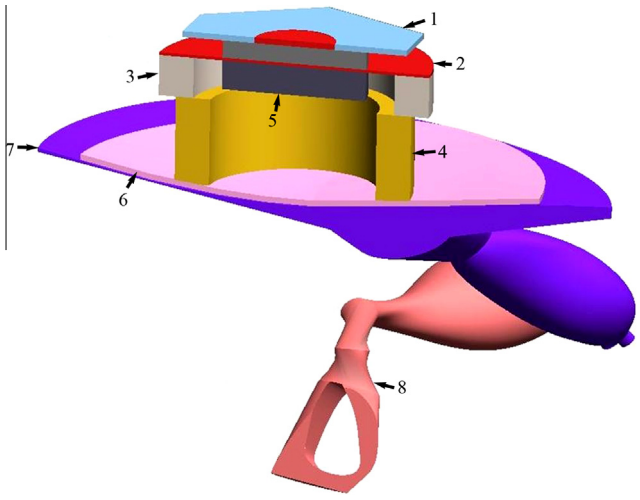

Fig. 1b. The components of the opto-electromagnetic vibration actuator include two photodiodes (1), a latex membrane (2), an aluminum ring (3), two oppositely wound coils (4), two permanent magnets (5) and a Provil Novo™ membrane (6). The tympanic membrane (7) and was connected to the ossicles (8).

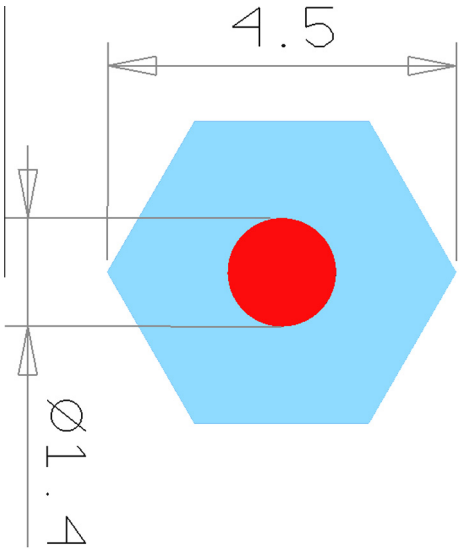

Fig. 2a. The novel design of the PD: the diameter of IR PD-2125 was 1.4 mm, and the maximum length of PD-5060 was 4.5 mm.

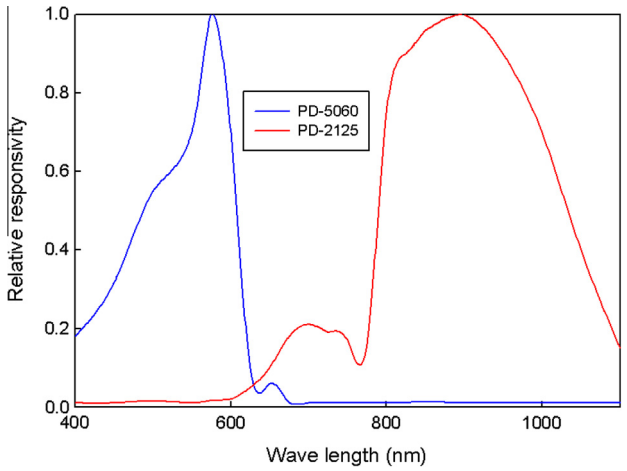

Fig. 2b. The spectra of PD-2125 and PD-5060 are shown.

coil. Hence, it was necessary to determine the structure, mass and size of the magnets, and the number of turns in the coil to determine the largest actuation force.

2.2. Force of the actuator

The vibration transducer was created by computer-aid design (CAD). The air gap between the magnet and the coil, the input current, and vibration force could be controlled by finite element (FE) simulation. A magnetic flux density around the permanent magnet was created, and the electromagnetic force generated by the coil current could be calculated.

Eq. (1) shows that the magnetic forces of the current in the magnetic field can be calculated with numerical integration [16]:

$$\{\mathrm{Fm}\} = \int \{N\}^T(\{\mathrm{Jc}\} \times \{\mathrm{Bm}\})d(vol) \quad (1)$$

where {Fm} is the vector matrix of Lorentz force, {Jc} is the vector matrix of current density, {Bm} is the vector matrix of magnetic flux density, and $\{N\}^T$ is the shape vector function.

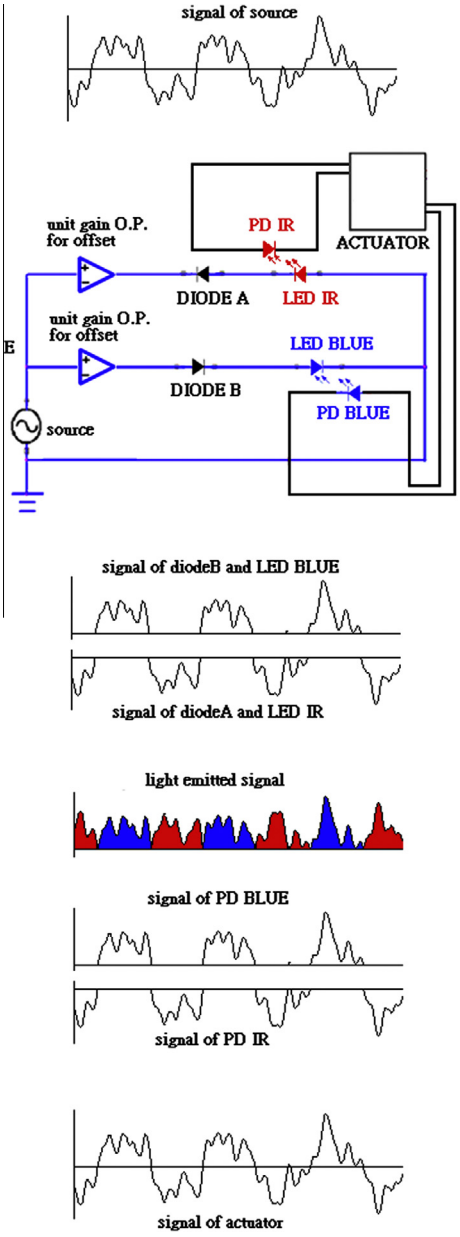

Fig. 2c. The diagram of two half-wave rectifiers: the positive cycles of the signals passed through the blue light emitting diode (LED-5060, BLUE) and were then received by the corresponding blue photodiode (PD-5060, BLUE). The negative cycles of the signals passed through the IR light emitting diode (LED-2125, RED) and were then received by the corresponding green photodiode (PD-2125, RED). Diodes A and B were used to avoid the inverse breakdown point of the LED and to ensure its durability. (For interpretation of the references to colour in this figure legend, the reader is referred to the web version of this article.)

2.3. Signal processing

An optic probe was designed to allow sound and light signals to enter the ear canal, thereby preventing the occlusion effect that is caused by traditional ear molds. The dimensions of the light probe were 40 cm in length and 0.76 mm^2 in cross-section area. The probe was designed to be inserted to pass the cartilaginous portion and reach the second portion of the external ear canal. The working distance between the probe tip and the actuator was approximately 10–15 mm. The probe could be shaped with package materials so that the orientation of the probe was adjustable and provided a direct incidence of light on the PD to minimize the effect of misalignment.

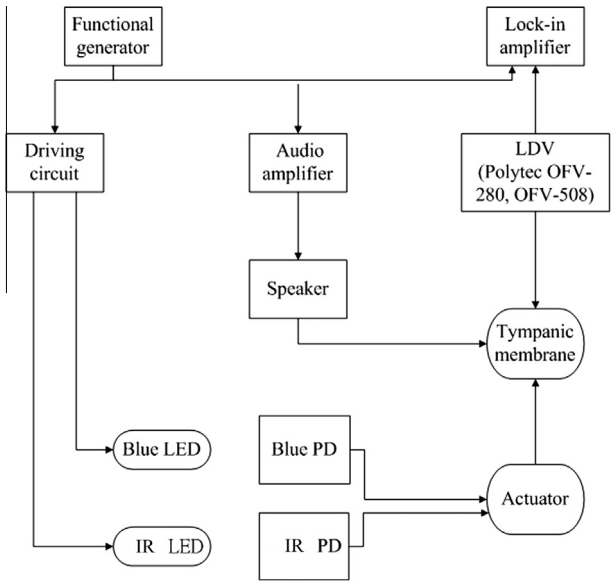

Fig. 3a. An illustration for measuring the displacement of the fabricated actuator.

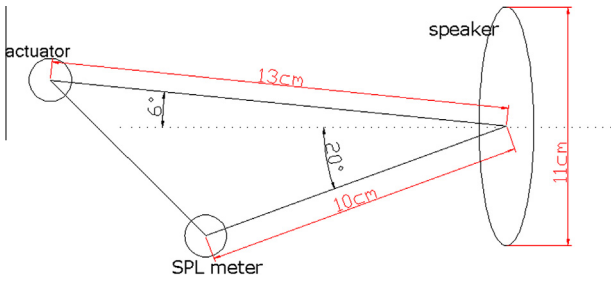

Fig. 3b. A schematic of the test system with a sound level meter, speaker and actuator.

Two LEDs were used (ED-5060 and ED-2125; OPTO TEC, Taiwan) to carry the input signals. The corresponding PDs were used (PD-5060 and PD-2125; OPTO TEC, Taiwan) to receive the light signals and generate the currents in the actuator [Fig. 2(a)]. As can be seen from the spectra of PD-2125 and PD-5060 in Fig. 2(b), the spectra of blue and infrared light are widely separated without overlapping, which means that the two output signals virtually do not influence each other. The maximum output current of the PD was approximately 280 μA. Two half-wave rectifiers were used to process the input signals. As two half-wave rectifiers to process the input signals in the LED were used, only one half of the current (approximately 140 μA) could be generated from the corresponding PD. The positive cycles of signals were passed through the blue LED and were then received by the corresponding blue PD. Similarly, the negative cycles of signals were passed through the infrared LED and were then received by the corresponding infrared PD. Because the actuator was composed of two bi-directionally wound coils, the magnetic fields created by the cycling currents were transformed into mechanical forces in the actuator. The actual voltage of the electrical signals was controlled below 3 V. Diodes A and B, which are shown in Fig. 2(c), were used to avoid the inverse breakdown point of the LED and to ensure its durability. The LED was used in its linear range by carefully adjusting the operation voltage of LED between 0 and 3 V.

2.4. Fabrication and testing of the actuator on the Dog temporal bone

The actuator was fabricated based on the results calculated by the FE model and adaptations of its original design. The mechanical and acoustic characteristics of the actuator were measured with a laser Doppler vibrometer (Polytec OFV-2802 and OFV-508, Karlsruhe, Germany). The sound source was a speaker (Pioneer, TS-01602R, USA) driven by a function generator, and a sound level meter (Rion NA-24, Japan) was used to measure and control the SPL at the TM. The test system used to measure the displacement of the fabricated actuator is shown in Figs. 3(a) and (b). A sound level meter was used to measure and control the SPL relative to the TM as our reference. Human cadaver temporal bone was obtained, and the actuator was placed on the TM. All measurements were recorded in a humid environment to control the degradation processes as described by Eiber et al. [17]. Fresh canine temporal bone was placed in a bone holder attached to a heavy metal plate, and a retro tap (Polytec, Karlsruhe, Germany) was glued to the umbo. The cochlea was subsequently extirpated from the posterior side to measure the vibration amplitudes of the umbo using posterior tympanotomy. Experiments were conducted in a dark room so that the equivalent input sound level of ambient light was negligible. To calculate the change in decibels correlated with the umbo displacement, we used the following equation [18]:

$$\delta\,\mathrm{dB} = 20\log(\mathrm{dexp}/\mathrm{dcontrol}) \tag{2}$$

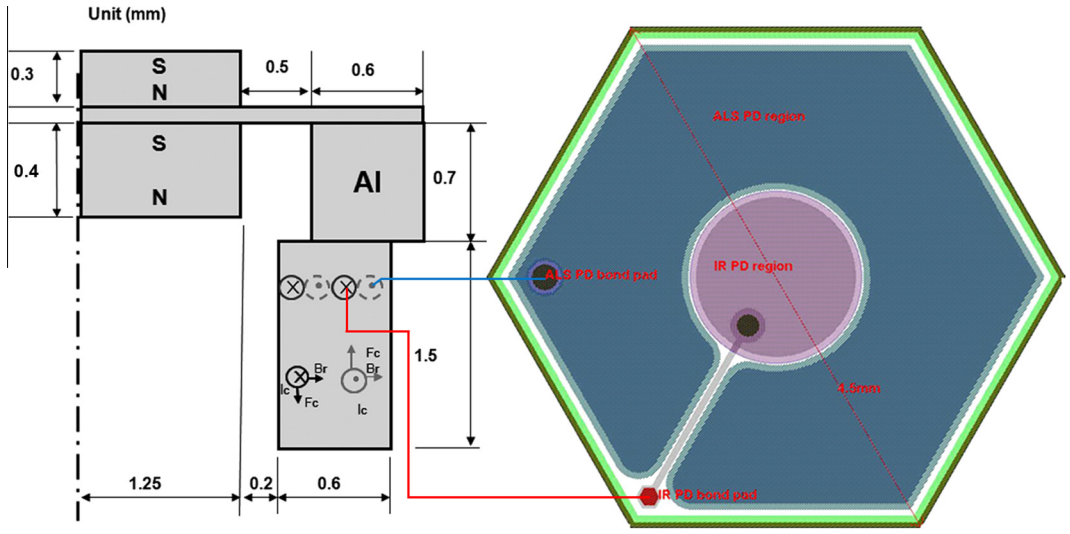

Fig. 3c. The electromagnetic driving part: a schematic diagram of the designed vibration actuator.

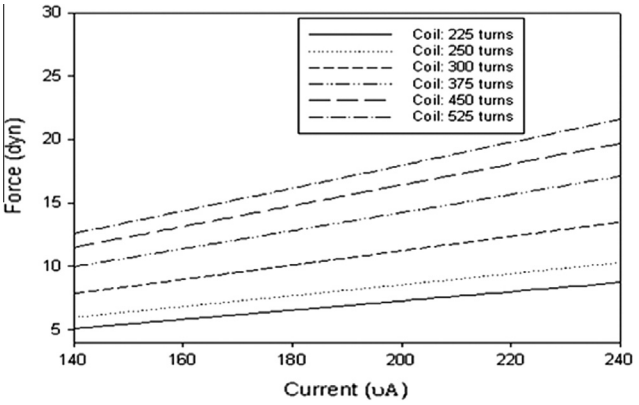

Fig. 4a. The simulation results of the vibration force vs. the input currents at the variance of turns of coil and the condition of a 200 μm air gap.

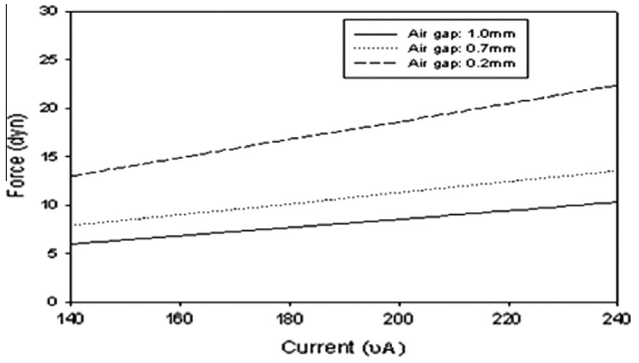

Fig. 4b. The simulation results of the vibration force vs. the input current at the variance of the air gap between the coil and magnet with 500 turns of coil.

In Eq. (2), δ dB is the change in decibels correlated with the umbo displacement that occurred after the actuator was placed on the ear drum; dexp and dcontrol are the umbo displacements measured in the actuator with different input currents and without current, respectively.

3. Results

3.1. Estimated force by FE model

The input sound level applied to the TM with the actuator was estimated from our previous middle ear model [16]. The mass of the actuator was approximately 95 mg, which included two permanent magnets, two wound coils, one aluminum ring, one latex membrane and two photodiodes (PDs). The electromagnetic driving parts were composed of two wound coils, an aluminum ring, a latex membrane and two permanent magnets, as shown in Fig. 3(c). The diameter and the thickness of the small permanent magnet were 2.5 and 0.3 mm, respectively. The diameter and the thickness of the large permanent magnet were 2.5 and 0.4 mm, respectively. The permanent magnets were a neodymium iron boron (NdFeB) metal alloy. The maximum magnetic flux density on the surface of the magnet was 2900 G. The air gap between the magnet and the coil was 200 μm. The wire diameter of the wound coil was 15 μm. FE analysis was performed to optimize the electromagnetic force.

The Lorentz forces between the coil and magnet as well as those between the turns of the wound coil are given in Fig. 4(a), with an air gap of 200 μm. Fig. 4(b) shows the magnetic forces observed when the air gaps are varied from 0.2 to 1 mm, with 500 turns of the wound coil. When the magnetic vibration actuator was

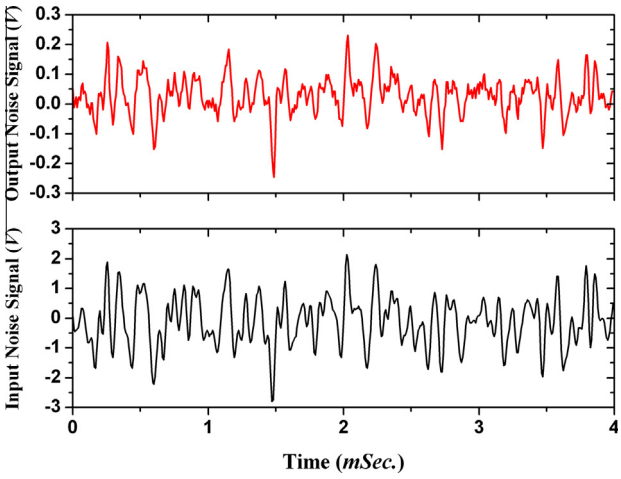

Fig. 5. The sound signal was input into the rectifier and then sent to the LED, and the composed sound signal output from the PD was demonstrated.

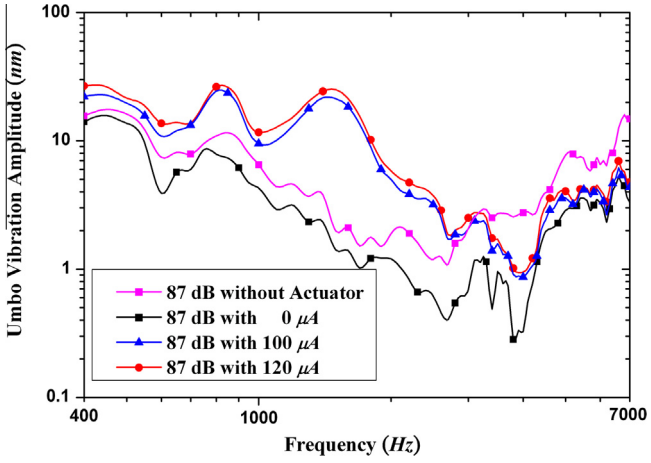

Fig. 6a. The *in vitro* experimental frequency response of the umbo driven with 87 dB SPL in the eardrum, and the frequency response of the fabricated actuator driven with currents of 100 μA and 120 μA.

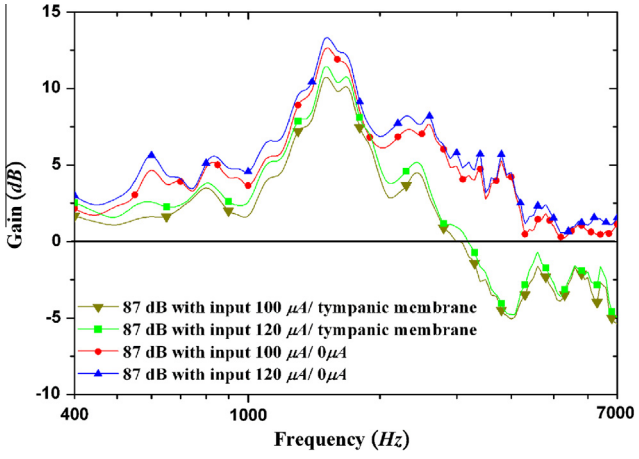

Fig. 6b. The gain of the umbo driven with 87 dB SPL in the eardrum, and the frequency response of the fabricated actuator driven with currents of 100 μA and 120 μA.

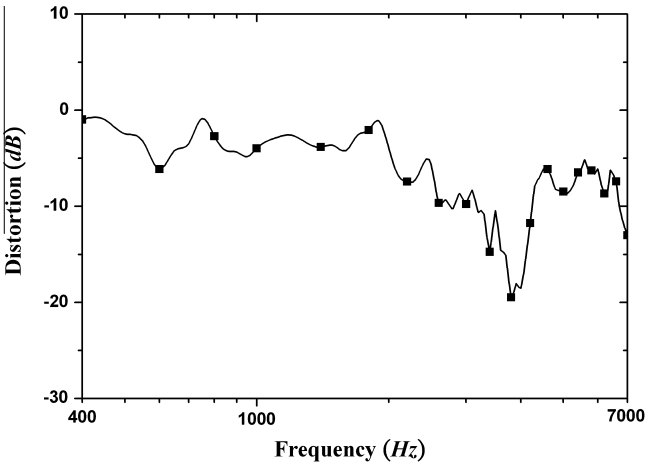

Fig. 6c. The distortion of the vibration amplitude of umbo vs. frequency.

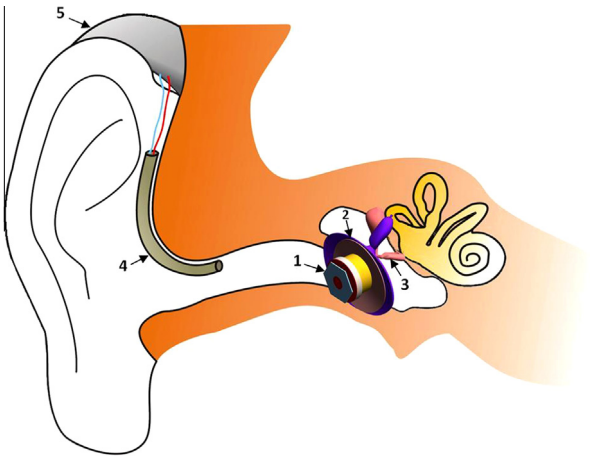

Fig. 7. A cartoon representation of the wireless actuator *in situ*. The actuator (1) coupled to the TM (2), and the ossicles (3). The light probe (4) and the behind-the-ear signal processor together as a complete amplification device (5).

fabricated according to the simulation results of Figs. 4(a) and (b), the actuator provided a force of 15 dyn. These results were observed under conditions that included 500 turns of each coil, 0.2 mm of air gap and a current of 160 μA. To obtain the maximum magnetic force of the actuator, we added an aluminum ring with an inner diameter of 3.5 mm, an outer diameter of 4.7 mm and a height of 0.7 mm.

3.2. Acoustic and mechanical measurements

The input sound signal and output signal elicited by white noise in the fabricated actuator are shown in Fig. 5. The two half-wave rectifiers were used to process the input signals and are shown in Fig. 2(c). The experimental results showed that the output vibration waveform correlated with the input sound signal current. The actuator with the new design was fabricated and was put onto the TM in fresh canine temporal bone. Figs. 6a–c shows the *in vitro* experimental frequency response of the umbo driven with 87 dB SPL in the eardrum and the frequency response of the fabricated actuator driven with currents of 100 μA and 120 μA. A first resonant frequency (RF) appeared near 800 Hz, the second RF occurred near 1500 Hz, and the third RF occurred near 3200 Hz. The fourth RF occurred near 5000 Hz, the fifth RF appeared at 5000 Hz, and the sixth RF occurred at 6500 Hz. The frequency response of the fabricated transducer indicated that the displacement of vibration is from 30 nm to 0.2 nm (at 400–7000 Hz) and decreases with higher frequencies. At frequencies near 3000 Hz, the vibration amplitudes of the actuator with different input currents were smaller than those of the tympanic membrane without a loading actuator. In our experiment, the gain of the actuator with 120 μA on the umbo displacement was approximately 3–13 dB (400–1500 Hz), 6 dB (1500–3000 Hz) and −1 to −6 dB (3000–7000 Hz) relative to the tympanic membrane, as shown in Fig. 6(b).

In our test conditions, the distortion of the output spectrum was −1 to −20 dB, which means that the vibration amplitude of the actuator without input current at 87 dB SPL relative to the tympanic membrane without a loading actuator. The distortion of the vibration amplitude of umbo vs. frequency is shown in Figs. 6(a)–(c). The distortion of the umbo vibration amplitude was approximately −1 to −10 dB (400–3000 Hz), −10 to −20 dB (3000–4200 Hz) and −6 to −10 dB (4200–7000 Hz). At a frequency of 3800 Hz, the maximum distortion was close to −20 dB. The distortion appears to be smaller at lower frequencies.

4. Conclusion

The inability to communicate because of hearing loss can be severely disabling. Predictably, only one in five individuals who stand to benefit from hearing aids acquires one, and a quarter of those patients do not wear a hearing aid because of problems with background noise and feedback phenomena [19]. In this study, an opto-electromagnetic vibration actuator that can leave the ear canal open was created and tested using the finite element method. An electromagnetic actuator could offer several advantages such as a high field energy density, a fast response time and a large deflection for low input voltage [20]. In the present study, the optimal

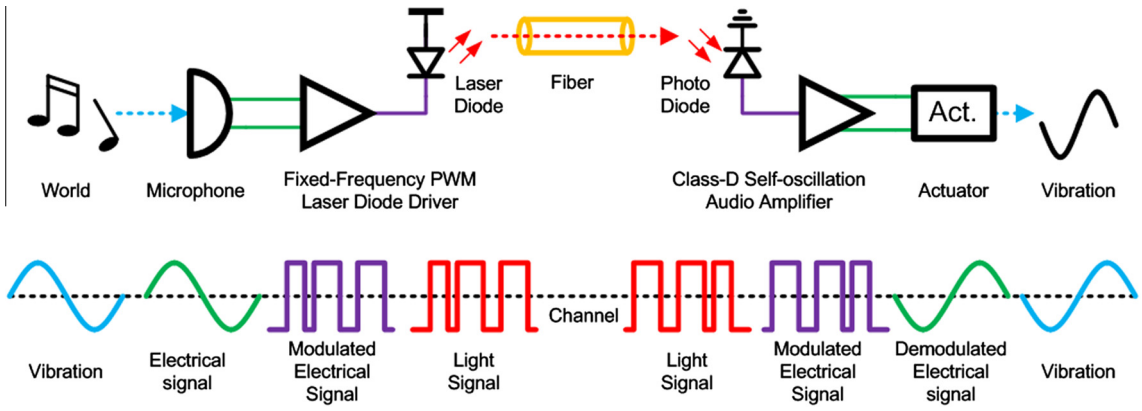

Fig. 8a. The audio wireless optical TX/RX system architecture.

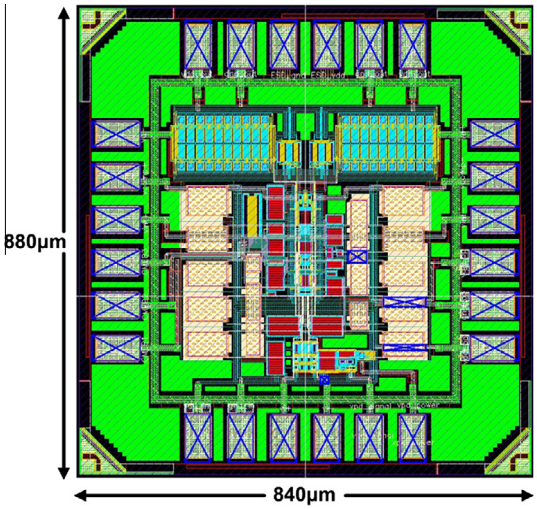

Fig. 8b. The chip layout 0.88 × 0.84 mm^2 in dimension. The chip will be made using TSMC 90 nm standard CMOS technology.

size and shape were determined by FE calculations. The configuration of this actuator offers several advantages over conventional hearing aids. The potential benefits include the elimination of feedback and occlusion and the direct drive of the ossicles. In addition, the open ear canal provides a pathway for the retention of normal resonances. The new type of actuator described in this study was placed on the umbo area of the TM, and its position was maintained with mineral oil. The conically concave shape of the TM and the adhesive forces required to maintain the device's position were entirely provided by the mineral oil, which eliminates the need for surgical installation for these patients. The results of this preliminary study suggest that adequate amplification can be achieved from this actuator.

The results of this preliminary study suggest that adequate amplification up to 3000 Hz can be achieved by this actuator. The frequency response indicated that the amplitude of displacement is 30 nm to 0.2 nm (at 400–7000 Hz) but is reduced at higher frequencies. At frequencies above 3000 Hz, the vibration amplitudes of the actuator under different currents (100–120 μA) are smaller than the amplitudes the tympanic membrane. The reduced amplitude was a consequence of the mass effect of the actuator at high frequencies. In this study, the mass of the wireless actuator was approximately 95 mg. Gan et al. reported that masses as little as 25 mg can cause attenuation of displacement of the ear drum [18]. The actuator created in this study is only a prototype. The first mode natural frequency of the actuator can use a simplified expression as $\omega_1 = \sqrt{k/m}$ without loss of generality. The reduction of mass can increase the natural frequency. The frequency response between eardrum displacement response and magnet excitation force in the frequency beyond ω_1 can be approximated as $1/m\omega^2$. Obviously, a smaller mass can result in a higher frequency response. Therefore, the gains at the frequency range higher than from 3.0 kHz can be improved by reducing the moving magnet mass. The usable bandwidth of actuator will then be improved. The gain of the actuator with 120 μA on the umbo displacement was approximately 3–13 dB relative to the tympanic membrane when the frequency was smaller than 3000 Hz. Further refinement and miniaturization are necessary for effective high frequency amplification.

Our experimental results showed that the output vibration waveform correlated with the input sound signal current. However, some differences in the output sound signal were noted. These differences may arise from the non-linear characteristics of the LED and the corresponding PD. The frequency responses of the actuator revealed multiple peaks in the response curve, and these peaks may be a consequence of the different vibration modes of the actuator systems in the middle ear. However, these peaks can be resolved and addressed with psychoacoustic tuning curves or by reshaping with the signal processor. The mass and size of the actuator can be reduced by using more powerful permanent magnets and more efficient PDs. In the future, we will conduct *in vivo* experiments in humans. Fig. 7 shows a cartoon representation of the wireless actuator *in situ*. In the future, our group will develop a novel wireless optical power transfer and actuator coupled to the tympanic membrane (Figs. 8(a) and (b)). The audio processor can convert the signal to a digital signal by a fixed-frequency pulse-width modulator (PWM) for the binary requirement for the laser diode driver to transmit the signal and power. An optical receiver is used to demodulate the current signal of the photo diode and to drive the actuator. Complementary metal–oxide–semiconductor (CMOS) is a technology for constructing integrated circuits and is used in microprocessors, microcontrollers, static random access memory (RAM) and other digital logic circuits. CMOS technology is also used for several analog circuits such as image sensors, data converters and highly integrated transceivers for many types of communication. A chip 0.88 × 0.84 mm^2 in dimension will be made in TSMC (Taiwan Semiconductor Manufacturing Company) using 90 nm standard CMOS (Complementary metal–oxide–semiconductor) technology.

Acknowledgements

This work was supported by a grant from the National Taiwan University Hospital to T.C.L. (Grant Numbers NTUH 95 A02 and 96 A01), a grant from the National Science Council to Y.F.C. (Grant Number NSC 95-2815-C-002-043-E) and a grant from the Buddhist Tzu Chi General Hospital to C.F.L. (Grant Numbers TCRD 9604 and 9607). We also appreciate Prof. Yeh L.S.'s (School of Veterinary Medicine National Taiwan University) help with the animal experiments.

References

[1] Kim KK, Barr DM. Hearing aids: a review of what's new. Otolaryngol-Head Neck Surg 2006;134:1043–50.
[2] Plomp R. Auditory handicap and the limited benefit of hearing aids. J Acoust Soc Am 1978;63:533–49.
[3] Arlinger S. Recent development in air-conduction hearing aids. Ear Nose Throat J 1997;76:310–5.
[4] Tode I, Seidl RO, Gross M, Ernst A. Comparison of different vibrant soundbridge audioprocessors with conventional hearing aids. Oto Neurotol 2002;23:669–73.
[5] Tjellstom A, Granstom G. Long-term follow up with bone-anchored hearing aid: a review of the first 100 patients between 1977 and 1985. Ear Nose Throat J 1994;73:112–4.
[6] Niehaus HH, Helms J, Müller J. Are implantable hearing devices really necessary. Ear Nose Throat J 1995;74:271–6.
[7] Perkins R. Earlens tympanic contact transducer: a new method of sound transduction to the human ear. Otolaryngol-Head Neck Surg 1996;114:720–8.
[8] MacKenzie DJ. Open-canal fittings and the hearing aid occlusion effect. Hearing J 2006;59:50–6.
[9] Killion MC, Wilber LA, Gudmundsen GI. Zwislocki was right a potential solution for the hollow voice problem (the amplified occlusion effect) with deeply sealed earmolds. Hear Instr 1988;39:14–8.
[10] Dillon H, Birtles G, Lovegrove R. Measuring the outcomes of a national rehabilitation program: normative data for the Client Oriented Scale of Improvement (COSI) and the Hearing Aid User's Questionnaire (HAUQ). J Am Acad Audiol 1999;10:67–79.
[11] Goode RL, Glattke T. Audition via electromagnetic induction. Arch Otolaryngol 1973;98:23–6.
[12] Wilska A. A direct method for determining threshold amplitudes of the eardrum at various frequencies. In: Kobrak HG, editor. The middle ear. Chicago: University of Chicago Press; 1959. p. 76–9.
[13] Wilska A. Ein method zur bestimmung der horsch wellenamplituden des trommelfells bei verschieden frequenzen. Skandiavisches Arch Physiol 1935;72:161–5.

[14] Gosalia K, Humayun MS, Lazzi G. Impedance matching and implementation of planar space-filling dipoles as intraocular implanted antennas in a retinal prosthesis. IEEE Trans Antennas Propag 2005;53:2365–73.
[15] Narayanan MV, Rizzo JF, Edell D, Wyatt JL. Development of a silicon retinal implant: cortical evoked potentials following focal stimulation of the rabbit retina with light and electricity. Invest Ophthal Vis Sci 1994;35:1380.
[16] Park S, Lee KC, Cho JH, Lee SH. Electromagnetic vibration transducer using polyimide elastic body for implantable middle ear hearing aid. Sens Actu A 2002;97:201–7.
[17] Eiber A, Kauf A, Maassen MM. First comparisons with laser vibrometry measurements and computer simulation of ear ossicle movements. HNO 1997;45:538–44.
[18] Gan RZ, Dyer RK, Wood MW. Mass loading on the ossicle and middle ear function. Ann Otol Rhinol Laryngol 2001;110:478–85.
[19] Kochkin S. The VA and direct mail sales spark growth in hearing aid market. Hear Res 2001;8:16–24.
[20] Kuckel H, Earles T, Klein J, Zook JD, Ohnstein T. Electromagnetic linear actuator with inductive position sensing. Sens Actu A 1996;53:386–91.